

Influence near-infrared ultrashort laser pulse duration on silicon ablation

© N.R. Lebedev^{1,2}, N.V. Minaev¹, V.I. Yusupov¹, S.I. Tsygina¹, E.I. Mareev¹

¹ National Research Nuclear University „MEPhI“, Moscow, Russia

² Kurchatov Complex Crystallography and Photonics, NRC „Kurchatov Institute“, Moscow, Russia

E-mail: mareev.evgeniy@physics.msu.ru

Received November 28, 2024

Revised March 12, 2025

Accepted March 20, 2025

By varying the duration and energy of ultrashort near-infrared laser pulses, it was demonstrated that the size of microstructuring on silicon surfaces, as well as the optical breakdown threshold, are primarily determined by the effects of avalanche ionization. The laser-induced microstructure consists of two zones: a central zone, which size logarithmically depends on the laser pulse energy E , and a peripheral area, whose size is proportional to $E^{1/2}$. These regions are characterized by different amounts of the crystalline phase of silicon. Using rate equations, it has been shown that this dependence is due to the increased contribution of avalanche ionization as the pulse duration changes from 200 fs to 2 ps (the breakdown threshold varies from ~ 0.2 to 0.22 J/cm^2).

Keywords: femtosecond laser ablation, rate equations, silicon.

DOI: 10.61011/TPL.2025.06.61298.20201

Silicon is one of the most abundant elements and serves as the basis for semiconductor technologies, playing a critical role in microelectronics, photovoltaics, and photonics [1,2]. However, being an indirect-gap semiconductor, it has limited efficiency, especially in solar cell production [1]. Lithographic technologies applied in silicon photonics are often used to improve its physical and chemical properties [3]. However, such approaches may limit the integration of photonic and electronic components on a single platform [4]. In this context, laser ablation is regarded as a promising alternative method for precise modification of the surface properties of silicon [5]. The efficiency of laser ablation depends largely on the ionization mechanism in the region of interaction of laser radiation with the material [6–9]. New possibilities for more precise control of the ablation process are opening up with the advent of ultrashort (i. e., femtosecond or picosecond) laser pulses [10]. However, many aspects of interaction of ultrashort pulses with silicon have not been studied yet. Such studies were carried out both experimentally [11,12] (by measuring the optical breakdown thresholds as a function of laser pulse duration) and theoretically [13] (using the rate equation for charge carriers and the two-temperature model). However, the influence of ionization mechanisms, which change with varying pulse duration, on the morphology of microstructuring has not been analyzed. Therefore, the aim of the present study is to analyze the influence of plasma generation mechanisms and the nature of changes in laser-induced microstructures on the silicon surface with variation of the energy and duration of laser pulses.

A TETA-20 (Avesta, Russia) femtosecond laser system operating at wavelength $\lambda = 1030 \text{ nm}$ was used to investigate the process of laser ablation of the silicon surface (100 KDB (3000-5000) [111] — 460 BPKZh 90.01.000 TU gr. C silicon wafers). The laser pulse duration

was varied (0.2–10 ps) by changing the position of the diffraction grating in the compressor. To vary the energy of laser radiation, it was passed through a $\lambda/2$ plate and a Glan prism mounted one after the other. Laser radiation was focused onto the silicon surface with an F-theta objective (NA = 0.1). The $1/e^2$ spot diameter on the silicon surface was $50 \mu\text{m}$, the beam displacement rate was 510 mm/s, the overlap coefficient (the ratio of the interpulse distance to the spot diameter) was 0.61, and the pulse repetition rate was 16.7 kHz. Linear arrays of structures were formed on the surface of silicon samples with different laser pulse energy or duration values. When a surface is ablated with ultrashort laser pulses with Gaussian (in space) profiles, the diameter of the modified (melted, damaged, ablated, etc.) region depends on the fluence as $D^2 = 2\omega^2 \ln(F/F_{th})$, where ω is the $1/e^2$ waist diameter on the surface, F is the energy density, and F_{th} is the threshold energy density of material modification [14]. The obtained microstructures were also examined by Raman spectroscopy. Spectral measurements were performed using a Nicolet Almega XR spectrometer with a 532 nm laser excitation source and a power up to 20 mW. The Stokes frequency shift components within the range of 250–600 cm^{-1} with a spectral resolution of 2 cm^{-1} were used for analysis.

Dynamic rate equations were used to model femtosecond laser breakdown. Applying these equations, one may characterize plasma density concentration ρ as [15]

$$d\rho/dt = v_{fi}\rho_u + \gamma_u\xi\rho - \gamma_r\rho.$$

Here, v_{fi} is the photoionization rate, γ_u is the rate of photon absorption by electrons at level u , γ_r is the recombination rate, and ξ may be written as $\xi = \text{erfc}(r) + 2r/\sqrt{\pi} \exp(-r^2)$, where $r = \sqrt{3E_c/2E_{kin}}$, E_c — critical energy, and E_{kin} — average kinetic energy of electrons with temperature T , $E_{kin} = 3k_bT/2$, and

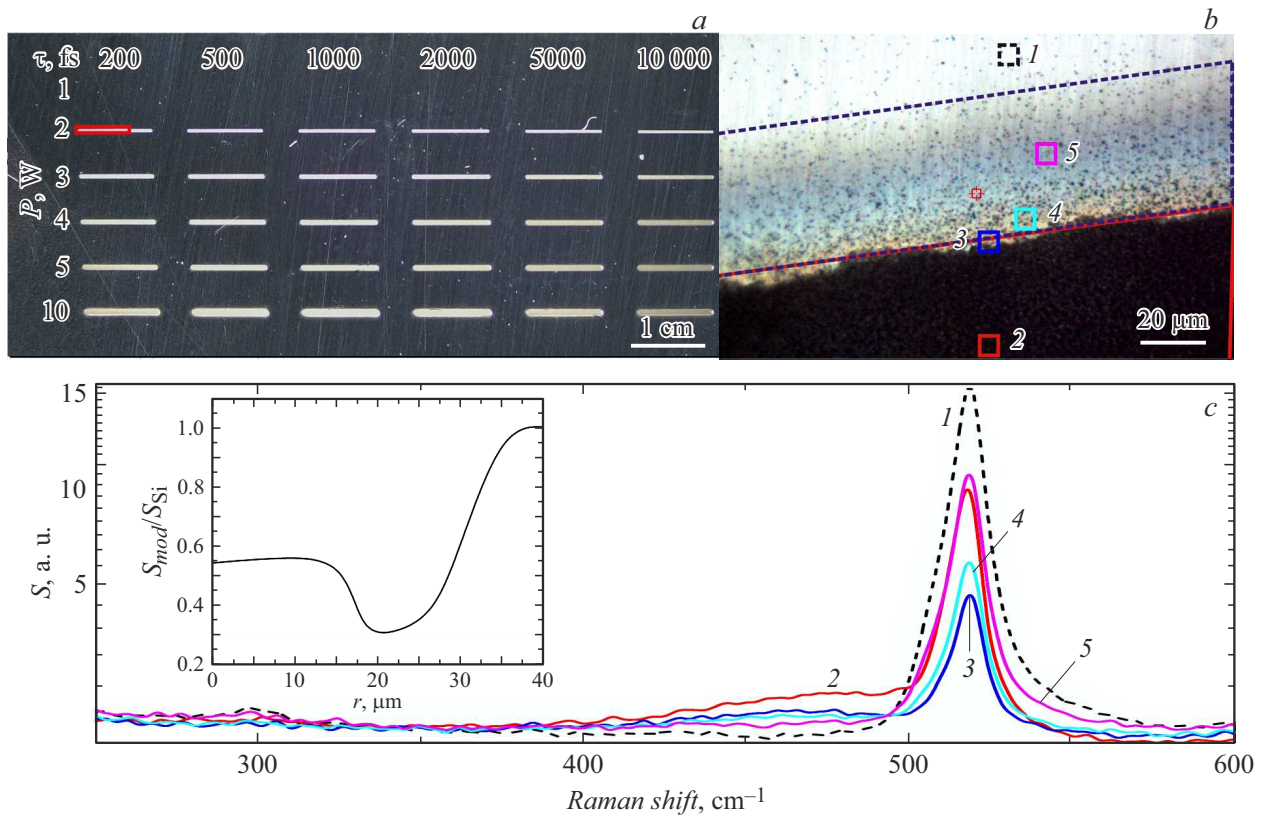


Figure 1. *a* — Microscopic images of the array of microstructures obtained with varying energy and duration of the laser pulse. *b* — Magnified image of the region of laser exposure (marked with a red rectangle in panel *a*). Colored squares 1–5 indicate the regions in which the Raman spectra presented in panel *c* were recorded. The red and black squares in panel *b* mark the central and peripheral zones of laser exposure. *c* — Raman spectra obtained at different distances from the center of laser exposure. The inset shows the relative values of amplitudes of the Raman signal at 521 cm^{-1} (i.e., the ratio of the Raman signal of modified silicon to the signal of unmodified silicon). A color version of the figure is provided in the online version of the paper.

k_b — Boltzmann constant. This model was discussed in more detail in [15]. The parameters from [6] were used in calculations.

When an intense ultrashort laser pulse is focused onto the surface of a semiconductor, laser radiation is absorbed due to the formation of electron-hole plasma with a high temperature. Ultra-fast melting is initiated when energy is transferred from plasma to the crystal lattice, and material ablation commences upon reaching the threshold intensities [16]; when laser radiation is switched off, the lattice temperature drops and the material recrystallizes [16]. In addition, new polymorphic phases (depending on the exposure regime) may be formed [2]. Arrays of microstructures were obtained experimentally at different values of energy density (fluence) and duration of a laser pulse (Fig. 1). The obtained microstructures were then analyzed by optical microscopy and Raman spectroscopy methods. The image of microstructures formed with different laser pulse parameters (Fig. 1, *a*) makes it clear that the dependence of their diameter is non-monotonic.

Let us consider the microstructure topology: the central region in its middle part has a pronounced black color. The

Raman spectra in this region reveal clearly a 400–500 cm^{-1} wing that is characteristic of amorphous silicon, while the total integral of Raman spectra is preserved. Notably, the amplitude of the peak at 521 cm^{-1} decreases significantly (Fig. 1), while the amplitude of the part of the spectrum characteristic of amorphous silicon increases. The minimum Raman signal intensity is observed at distances of 20–30 μm from the crater center, which may be attributed to increased scattering at the boundaries. Outside the crater, the Raman signal amplitude returns to its original level. The outer layer at the boundaries of the central region has a pronounced blue-violet hue in optical images (Fig. 1, *b*). This may be attributed to the shift of the absorption spectrum of amorphous and microcrystalline silicon to the visible region (compared to crystalline silicon) and to the formation of a thin oxide film, which causes the color to change slightly under observation at different angles [17]. Comparing the amplitudes of the Raman signal at 521 cm^{-1} , one can see that the amount of crystalline silicon at the periphery is smaller than the corresponding amount at the center (see the inset in Fig. 1, *c*). This is likely attributable

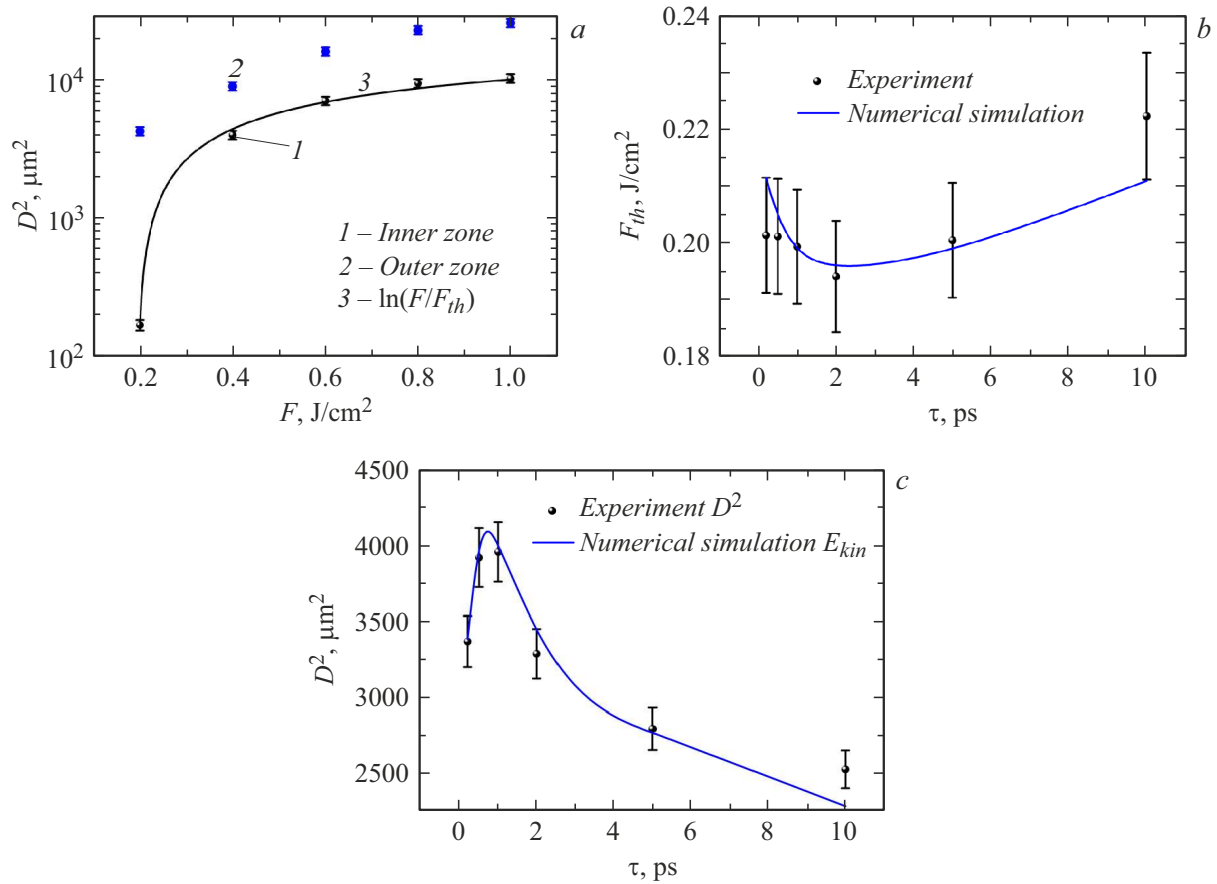


Figure 2. *a* — Dependences of the squares of microstructure diameters on the energy density (fluence) for the central and peripheral regions ($\tau = 500$ fs). The solid curve is the logarithmic approximation. *b* — Dependence of the microstructure formation threshold on the laser pulse duration. The solid curve is the result of numerical simulation. *c* — Dependence of the squares of microstructure diameters in the peripheral region on the laser pulse duration ($F \sim 0.4 \text{ J}/\text{cm}^2$). The solid curve represents the total kinetic energy of plasma reduced to the values of diameter squared at 200 fs.

to the difference in rates of temperature relaxation at the center and at the edges of the microstructure.

Approximating the dependence of the squared diameter of the microstructure on the silicon surface on energy density by a logarithmic function, one may determine the threshold values for each duration (see above; Fig. 2, *a*). The data obtained this way agree, within the error limits, with the energies at which cratering ceased to be visible. If the dependence of the square of the central region diameter on energy density is characterized well by a logarithmic function (which is consistent with literature data, since such a dependence stems from the Gaussian profile), then the squared diameter of the peripheral region increases almost linearly with increasing energy density. The silicon structure in this region contains less crystalline silicon, indicating that the lattice temperature was, at the very least, above the melting point. Thus, it can be assumed that the diameter of this region is determined by the energy deposited in the lattice.

To gain a better understanding of this dependence, one needs to consider the dynamics of laser-induced plasma,

since energy is transferred to the lattice in two stages: the energy of a laser pulse is first absorbed by plasma and only then is transferred to the lattice through electron-phonon interaction. Since relatively long (more than 200 fs) laser pulses were used in the present study, avalanche ionization played a critical role even at low energies (Fig. 3). An increase in laser pulse duration leads to an increase in efficiency of avalanche ionization. However, when the duration of a laser pulse starts exceeding the carrier recombination time in silicon (on the order of 1 ps), the electron concentration decreases at the trailing edge of the pulse. It should also be noted that avalanche ionization is „triggered“ in the presence of seed electrons, which are produced by photoionization (multiphoton and tunneling). The result is that an extremum forms in the dependence of the breakdown threshold on pulse duration (Fig. 2, *b*). This is related to the fact that an optimum ratio between photoionization and avalanche ionization is established at ~ 2 ps: a sufficient number of seed electrons are still being generated and avalanche ionization is extremely efficient.

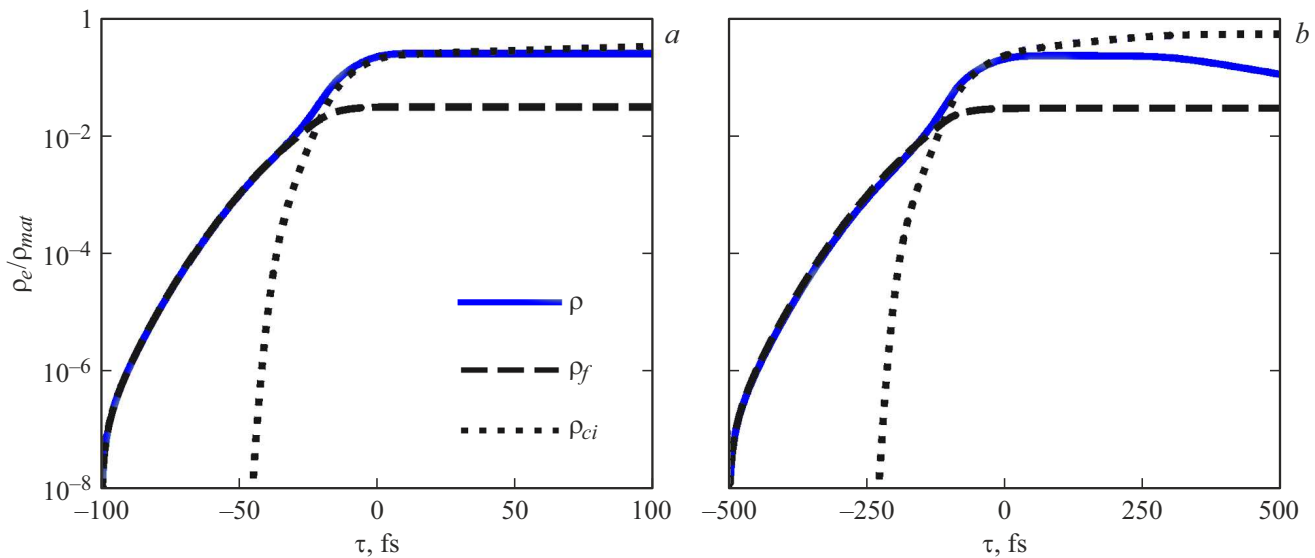


Figure 3. Dynamics of variation of concentration of laser-induced plasma for a laser pulse duration of 200 (a) and 1000 fs (b) at $F = 0.5 \text{ J/cm}^2$. The dashed, dotted, and solid curves represent the contribution of photoionization (without recombination), the contribution of avalanche ionization (without recombination), and the total contribution with recombination.

The model also allows one to calculate the total kinetic energy of plasma by multiplying the concentration of charge carriers by their temperature. The dependence of this energy (multiplied by a fixed coefficient for ease of presentation) is shown in Fig. 2, c. It can be seen that the dependence of the squared diameter of the peripheral region on laser pulse duration matches qualitatively the experimental one, indicating that it is the energy transferred from a laser pulse to plasma that determines the temperature and the area of laser exposure.

Thus, it was demonstrated that the variation of duration of ultrashort laser pulses at a wavelength of 1030 nm with soft focusing ($\text{NA} = 0.1$) leads to the emergence of an extremum in the dependences of dimensions of the region of laser exposure and the optical breakdown threshold on this duration. The obtained results revealed that laser-induced microstructuring of silicon includes two zones: the central one with its size depending logarithmically on laser pulse energy E and the peripheral region, the diameter of which increases proportionally to $E^{1/2}$. The lowest breakdown threshold and the maximum damage diameter were achieved at pulse durations of 1–2 ps, indicating that the optimum laser ablation conditions were established within this range. Rate equations were used to demonstrate analytically that this dependence is due to an enhancement of the contribution of avalanche ionization with an increase in pulse duration from 200 fs to 2 ps.

Funding

The experiments on laser irradiation of the silicon surface and microscopy studies were supported by grant 23-73-00039 from the Russian Science Foundation. The

work on numerical modeling was supported by the state assignment of National Research Center „Kurchatov Institute“ in respect of the provision of equipment of the „Structural Diagnostics of Materials“ common use center of the Kurchatov Crystallography and Photonics Complex (National Research Center „Kurchatov Institute“).

Conflict of interest

The authors declare that they have no conflict of interest.

References

- [1] H. Zhang, H. Liu, K. Wei, O.O. Kurakevych, Y. Le Godec, Z. Liu, J. Martin, M. Guerrette, G.S. Nolas, T.A. Strobel, *Phys. Rev. Lett.*, **118** (14), 146601 (2017). DOI: 10.1103/PhysRevLett.118.146601
- [2] S. Wippermann, Y. He, M. Vörös, G. Galli, *Appl. Phys. Rev.*, **3** (4), 040807 (2016). DOI: 10.1063/1.4961724
- [3] M.S. Kim, A.C. Assafrao, T. Scharf, A.J.H. Wachters, S.F. Pereira, H.P. Urbach, M. Brun, S. Olivier, S. Nicoletti, H.P. Herzig, *New J. Phys.*, **14**, 103024 (2012). DOI: 10.1088/1367-2630/14/10/103024
- [4] O. Tokel, A. Turnall, G. Makey, P. Elahi, T. Çolakoğlu, E. Ergeçen, Ö. Yavuz, R. Hübner, M. Zolfaghari Borra, I. Pavlov, A. Bek, R. Turan, D.K. Kesim, S. Tozburun, S. Ilday, F.Ö. Ilday, *Nat. Photon.*, **11** (10), 639 (2017). DOI: 10.1038/s41566-017-0004-4
- [5] M. Garcia-Lechuga, N. Casquero, J. Siegel, J. Solis, R. Clady, A. Wang, O. Utéza, D. Grojo, *Laser Photon. Rev.*, **18** (11), 2301327 (2024). DOI: 10.1002/lpor.202301327
- [6] E. Mareev, A. Pushkin, E. Migal, K. Lvov, S. Stremoukhov, F. Potemkin, *Sci. Rep.*, **12**, 7517 (2022). DOI: 10.1038/s41598-022-11501-4

- [7] K.V. Lvov, F.V. Potemkin, S.Y. Stremoukhov, *Mater. Today Commun.*, **35**, 105594 (2023). DOI: 10.1016/j.mtcomm.2023.105594
- [8] V.S. Popov, *Phys.-Usp.*, **47** (9), 855 (2004). DOI: 10.3367/UFNr.0174.200409a.0921 [V.S. Popov, *Phys. Usp.*, **47** (9), 855 (2004). DOI: 10.1070/PU2004v047n09ABEH001812].
- [9] E.I. Mareev, A.V. Pushkin, F.V. Potemkin, *J. Surf. Investig.*, **18** (Suppl. 1), S78 (2024). DOI: 10.1134/S1027451024701891
- [10] P. McKearney, S. Schäfer, X. Liu, S. Paulus, I. Lebershausen, B. Radfar, V. Vähänissi, H. Savin, S. Kontermann, *Adv. Photon. Res.*, **5** (6), 2300281 (2024). DOI: 10.1002/adpr.202300281
- [11] T. Takahashi, S. Tani, R. Kuroda, Y. Kobayashi, *Appl. Phys. A*, **126** (8), 581 (2020). DOI: 10.1007/s00339-020-03754-5
- [12] N.A. Smirnov, S.I. Kudryashov, P.A. Danilov, A.A. Rudenko, A.A. Ionin, A.A. Nastulyavichus, *JETP Lett.*, **108** (5-6), 368 (2018). DOI: 10.1134/S002136401818011X.
- [13] P. Allenspacher, B. Hüttner, W. Riede, *Proc. SPIE*, **4932**, 358 (2003). DOI: 10.1117/12.472053
- [14] J.M. Liu, *Opt. Lett.*, **7** (5), 196 (1982). DOI: 10.1364/ol.7.000196
- [15] J.L. Déziel, L.J. Dubé, C. Varin, *Phys. Rev. B*, **104** (4), 045201 (2021). DOI: 10.1103/PhysRevB.104.045201
- [16] J. Liu, M. Wu, Z. Sun, Q. Zhang, Y. Zhu, Y. Fu, *Appl. Surf. Sci.*, **661**, 160022 (2024). DOI: 10.1016/j.apsusc.2024.160022
- [17] A. Feltrin, R. Bartlomé, C. Battaglia, M. Boccard, G. Bugnon, P. Bühlmann, O. Cubero, M. Despeisse, D. Dominé, F.-J. Haug, F. Meillaud, X. Niquille, G. Parascandolo, T. Söderström, B. Strahm, V. Terrazzone, N. Wyrsh, C. Ballif, *Inform. MIDEM*, **39** (4), 231 (2009). [https://www.midem-drustvo.si/journal_papers/MIDEM_39\(2009\)4p231.pdf](https://www.midem-drustvo.si/journal_papers/MIDEM_39(2009)4p231.pdf)

Translated by D.Safin